Continuum percolation of isotropically oriented circular cylinders

D. Sangare and P. M. Adler*
UPMC Sisyphe, Boîte 105, 4 Place Jussieu, 75252 Paris Cedex 05, France
(Received 6 February 2009; published 13 May 2009)

The continuum percolation of circular cylinders has been studied for various values of the aspect ratio b'. The percolation threshold is shown to have a maximum for $b' \approx 2$ when the cylinder length is equal to its diameter. Other quantities such as the average intersection volume and the porosity also possess a maximum for this value.

DOI: 10.1103/PhysRevE.79.052101 PACS number(s): 64.60.ah, 02.50.−r

The study of the macroscopic properties of fractured media is of large academic and practical interests; among the possible applications are underground flow of fluids such as water and oil and the storage of nuclear wastes. Generally speaking, fractures are modeled as convex flat surfaces [1], but one may consider the case of fractures whose apertures are not negligible with respect to their lateral extension.

The simplest way of modeling such thick fractures is to study the properties of hollow circular cylinders of radius R and length b. An immediate difficulty arises since the percolation threshold $\rho_c(b')$ obtained for isotropically oriented capped cylinders [2] for values of $b'=b/R$ larger than 3 is a decreasing function of b'; moreover, ρ_c $(b'=3)$ is larger than the value obtained for flat convex surfaces [3,4], i.e., for $b'=0$.

Therefore, one of the initial objectives of this study was to reconcile these apparently contradictory results. In addition, the overall porosity of a population of hollow cylinders is expanded as a function of the number of cylinders per unit volume and successfully compared to numerical data. Finally, the porosity at the percolation threshold is estimated.

A key concept which rationalizes the results relative to percolation is the excluded volume which was introduced in the fracture field by [5]. For a pair of objects F_1 and F_2, with given shapes and orientations, the excluded volume V_{ex} is the volume in which the center of F_2 must be relative to the center of F_1 in order for F_1 and F_2 to intersect. For instance, if F_1 and F_2 are spheres with radii R_1 and R_2, the excluded volume is a sphere with radius R_1+R_2. It is recalled in [1] that if the objects are two dimensional, with areas A_i, perimeters P_i $(i=1,2)$, random orientations, and convex contours, their excluded volume is

$$V_{ex,12} = \frac{1}{4}(A_1P_2 + A_2P_1). \tag{1}$$

If all the polygons are identical, Eq. (1) reduces to

$$V_{ex} = \frac{1}{2}AP. \tag{2}$$

This is a particular case of the kinematic formula for convex bodies [6–8]. Let C_1 and C_2 be two convex bodies of surfaces S_i, average curvature M_i, and volume V_i $(i=1,2)$. Then, the excluded volume is given by

$$V_{ex} = V_1 + V_2 + \frac{1}{4\pi}(M_1S_1 + M_2S_2). \tag{3}$$

For two identical cylinders, Eq. (3) is simplified to

$$V_{ex} = \pi^2R^3\left(1 + \frac{3+\pi}{\pi}b' + \frac{1}{\pi}b'^2\right). \tag{4}$$

Note that for $b'=0$, Eq. (4) implies Eq. (2) evaluated for circular disks. Moreover, V_{ex} is an increasing function of b' for $b'>0$.

Let ρ be the object density, i.e., the number of objects per unit volume whether they are convex volumes or surfaces. V_{ex} may be used to define the dimensionless object density ρ',

$$\rho' = \rho V_{ex}. \tag{5}$$

ρ' can be interpreted as a volumetric density since it is the number of objects per volume V_{ex}; however, ρ' also represents the mean number of intersections per object with other objects in the network and, as such, it is a direct measure of the connectivity. Therefore, the number of intersections per unit volume ρ_I is given by

$$\rho_I = \frac{1}{2}\rho^2V_{ex}. \tag{6}$$

The factor of 1/2 is due to the fact that the total number of intersections is equal to half the number of intersections per object multiplied by the number of objects.

This definition proved very successful in unifying the critical densities of networks of fractures with different shapes. For regular polygons with 3–20 vertices, as well as for rectangles with an aspect ratio of 2 [3], we obtained a nearly constant percolation threshold,

$$\rho_c'(b') = 2.26 \pm 0.04, \tag{7}$$

a result in apparent contradiction with [2], as already mentioned.

In order to resolve this contradiction, N randomly distributed cylinders of radius R and length b are generated in a cubic domain Ω of size L with spatially periodic boundary conditions. Let $\mathbf{n}$ be the unit vector parallel to the axis of the cylinders. $L'=L/R$ is the dimensionless size of Ω. Cylinder centers are uniformly distributed in space and $\mathbf{n}$ is uniformly

*pierre.adler@upmc.fr

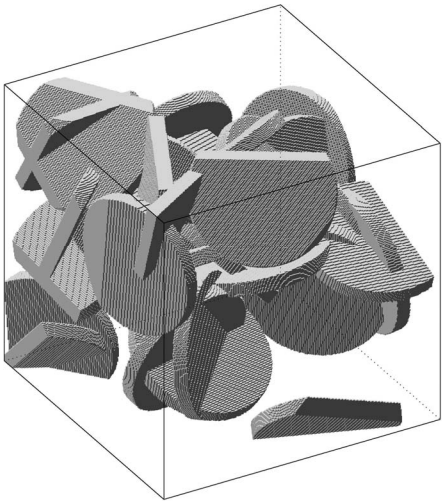

FIG. 1. Network of cylinders. Data are for $N_c=256$, $\rho'=4$, $R=60a$, and $b=12a$.

distributed on the unit sphere. For porosity measurements, Ω is discretized into N_c^3 elementary cubes of size $a=L/N_c$; N_c is typically on the order of 256. An example is given in Fig. 1.

The first step consists in the determination of the intersection of cylinders i and j $(j<i;\ \ i,j=1,\ldots,N)$ by following the procedure of [9]. Moreover, the spatial periodic character of the unit cell and of the network is taken into account as detailed by [3]. A graph Γ_1 is built whose vertices correspond to the cylinders and whose edges correspond to the intersections of the cylinders. The percolating character of Γ_1 along one of the three spatial axes is determined as in [3].

For each realization of the network, percolation is investigated along the three axes. In all the tests, $N_r=500$ realizations of the system are generated, from which the probability $\Pi(\rho',b',L')$ of having a percolating cluster is derived. The percolation threshold $\rho_c'(b',L')$ is estimated as the value for which $\Pi=0.5$.

In the limit of large L', the cylinder networks are expected to follow the standard percolation theory with the percolation threshold $\rho_c'(b',\infty)$, [10]

$$\rho_c'(b',L')-\rho_c'(b',\infty)\propto L'^{-1/\nu}, \tag{8}$$

where ν is the critical exponent. In our estimations of $\rho_c'(b',L')$, the data for $\Pi(\rho',b',L')$ were fitted by a two-parameter error function of the form

$$\Pi(\rho',b',L')=\frac{1}{\sqrt{2\pi}}\int_{-\infty}^{\rho'}\frac{1}{\Delta_L}\exp\left[-\frac{[\xi-\rho_c'(L')]^2}{2(\Delta_L)^2}\right]d\xi, \tag{9}$$

where Δ_L is the width of the transition region of $\Pi(L',\rho')$ which follows a scaling relation in the limit of large L',

$$\Delta_L\propto L'^{-1/\nu}. \tag{10}$$

When L' increases, Δ_L tends to zero. Therefore, in infinite systems, Π switches abruptly from 0 to 1 when ρ exceeds some critical density and percolation is a critical phenomenon.

The numerical results relative to the percolation threshold can be summarized as follows. First, the approximation by an error function was systematically verified and it was found to be very good. Second, the extrapolation process to infinite unit cells is also precise as shown by Fig. 2(a) for $b'<2$; similar results were obtained for $b'>2$. The extrapolated values of the percolation threshold $\rho_c'(b',\infty)$ are displayed in Fig. 2(b) where they are compared to the results of [2]. Two remarks can be obviously done. First, our results are in very good quantitative agreement with [2] for $b'>2$; second, for $b'<2$, $\rho_c'(b',\infty)$ is an increasing function of b'.

Therefore, the apparent contradiction which motivated this work is solved. The existence of a maximum in this curve for $b'\approx 2$ went un-noticed to the best of our knowledge.

It is also important to remark that the dimensionless percolation threshold depends on the shape of the three-dimensional objects considered in this work. This is in strong contrast to the findings for two-dimensional objects which were studied in [4]; the numerical studies showed that ρ_c' is almost independent of the fracture shape.

Another interesting point is the existence of a maximum for $b'\approx 2$ which corresponds to a length exactly equal to the diameter of the cylinders. The curve is quite spiky at the chosen scale. Moreover, the sphericity index ψ which is defined as the ratio between the surface of the sphere of the same volume and the surface of the cylinder is equal to

$$\psi=2\left(\frac{3}{4}\right)^{2/3}\frac{b'^{2/3}}{1+b'}. \tag{11}$$

It is easily shown that ψ is maximum for $b'=2$. Let us now evaluate the porosity of the system for N identical void cylinders thrown at random in Ω up to the second order of the fracture density. The first approximation ε_o consists in add-

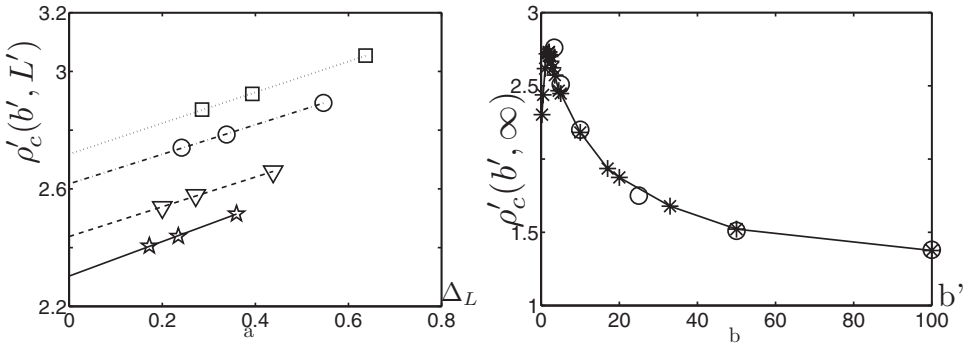

FIG. 2. The percolation threshold. (a) The percolation threshold $\rho_c'(b',L')$ as a function of the width of the transition region Δ_L for various b'. Data are for $b'=0.2$ ($\star$), 0.5 ($\triangledown$), 1 ($\bigcirc$), 1.5 ($\square$). (b) The extrapolated values of $\rho_c'(b',\infty)$ as a function of the dimensionless cylinder length b'; data of Neda *et al.* [2] ($\circ$)

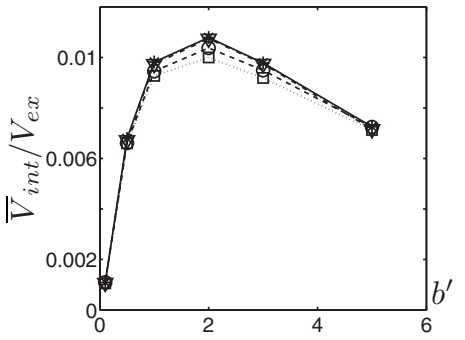

FIG. 3. The average intersection volume $\bar{V}_{int}$ as a function of the dimensionless cylinder length b' for a fixed number of intersections N_i. Data are for N_i=1000 (□), 2000 (○), 5000 (∗), and 10 000 (▽).

ing the volumes $V_{cyl}=\pi R^2 b$ of all the cylinders and this yields

$$\varepsilon_o = N\frac{V_{cyl}}{L^3}. \tag{12}$$

A more precise approximation ε_1 can be derived by subtracting the intersections between pairs of cylinders. The average volume of intersection between two cylinders is denoted by $\bar{V}_{int}$. The average number of intersections per cylinder is equal to ρ'. Therefore, the total pore volume is equal to

$$V_{pore} = NV_{cyl} - \frac{N}{2}\rho V_{ex}\bar{V}_{int}. \tag{13}$$

The resulting porosity ε_1 is the ratio between the pore volume and the volume of the unit cell,

$$\varepsilon_1 = \frac{V_{pore}}{L^3} = \frac{N}{L^3}V_{cyl} - \frac{1}{2}\frac{N}{L^3}\rho V_{ex}\bar{V}_{int}. \tag{14a}$$

Equivalently,

$$\varepsilon_1 = \rho V_{cyl} - \frac{1}{2}\rho^2 V_{ex}\bar{V}_{int}. \tag{14b}$$

A dimensionless formula can be easily derived as

$$\varepsilon_1 = \rho'\frac{V_{cyl}}{V_{ex}} - \frac{\rho'^2}{2}\frac{\bar{V}_{int}}{V_{ex}}. \tag{14c}$$

The practical use of this formula necessitates the knowledge of $\bar{V}_{int}$ which can only be obtained numerically. This is done in the following way. A cylinder is located in the center of a cell of size $4(R^2+b^2/4)^{1/2}$. Another cylinder is generated at random inside this cell; the size of the cell is large enough to include all the centers of the cylinders which can intersect the cylinder located at its center. Whenever it intersects the first cylinder, the two cylinders are discretized into small cubes of side a and the intersection volume is determined. $\bar{V}_{int}$ is obtained by averaging over a large number N_i of intersections

$$\bar{V}_{int} = \frac{1}{N_i}\sum_{i=1}^{N_i} V_i. \tag{15}$$

Calculations were done for N_i=1000, 2000, 5000, and 10 000 for each value of b'. Figure 3 displays the corresponding results when $\bar{V}_{int}$ is made dimensionless by V_{ex}. The numerical values for $\bar{V}_{int}$ converge rapidly and almost identical values are obtained for N_i=5000 and 10 000.

It is interesting to notice that the dimensionless intersec-

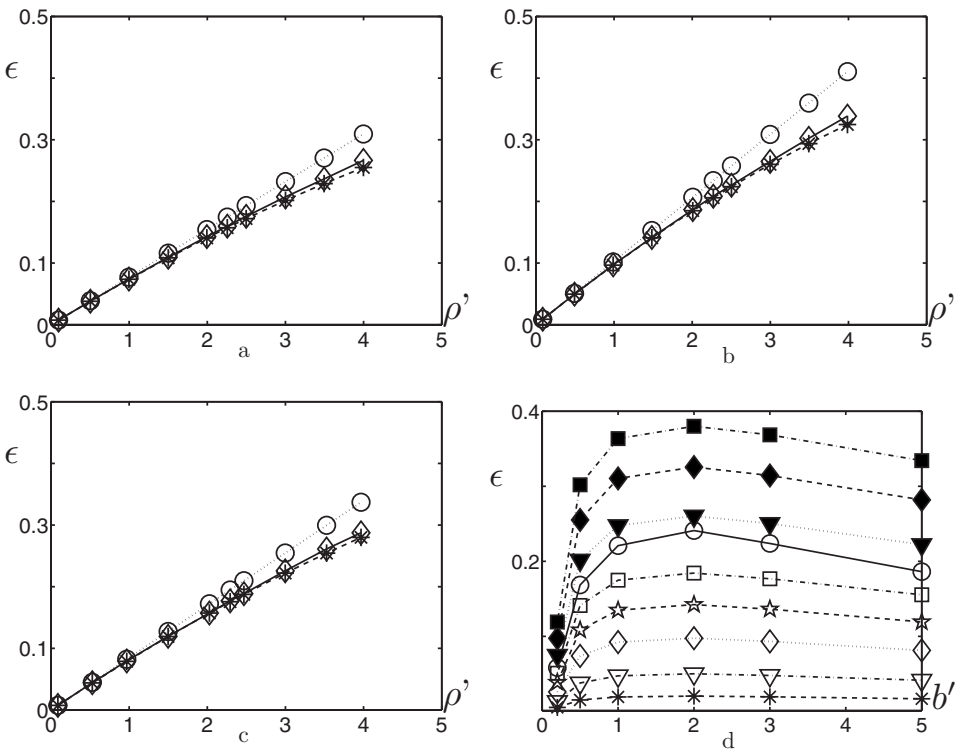

FIG. 4. (a)–(c) The average porosity as a function of the dimensionless density ρ'; data are for ε_d (16) (◇), ε_o (12) (○), and ε_1 (14c) (∗); subfigures are for b'=0.5 (a), 2 (b), and 5 (c). (d) The porosity as a function of the dimensionless cylinder length b' for various values of the cylinder density ρ'; data are for ρ'=0.2 (∗), 0.5 (▽), 1.0 (◇), 1.5 (⋆), 2.0 (□), ρ'_c (○), 3.0 (▼), 4.0 (♦), and 5.0 (■).

tion volume has a maximum for values of b' close to 2 as $\rho'(b',\infty)$ and ψ. The porosity of a network of random cylinders can be easily determined by discretizing the unit cell in which the cylinders are generated into elementary cubes. Since each elementary cube of size a is either solid or void, the porosity is obtained by

$$\varepsilon_d = \frac{n_v}{N_c^3}. \tag{16}$$

where n_v is the total number of void cubes.

In order to compare the three formulas (14), (12) and (16), N_r unit cells are generated and the porosity ε_d is determined and averaged. Calculations were systematically performed for $b'=0.1$, 0.5, 1, 2, 3, and 5.

Some of the results are illustrated in Figs. 4(a)–4(c) for three representative values of b'. Since the expansion in terms of ρ' is alternate, it is logical that ρ' overestimates Eq. (16) while Eq. (14c) underestimates it.

The major result of these calculations is that porosity is precisely estimated by expansion (14c) for all b' and for ρ' smaller than 3, i.e., for densities smaller than the percolation thresholds displayed in Fig. 2(b). Another way to display these results is given in Fig. 4(d) which provides porosity as a function of b' for various values of ρ'. Note that one curve is obtained at percolation, i.e., for a variable density. All these curves have a maximum for again b' close to 2. This maximum is slightly different for the curve obtained at percolation.

This study can be concluded as follows. The dimensionless percolation threshold, the average intersection volume, and the sphericity index are nonmonotonic functions of the aspect ratio b' of circular cylinders. Moreover, in contrast to previous results obtained for plane convex polygons [3,4], ρ_c' depends on the shape of the cylinders.

[1] P. M. Adler and J.-F. Thovert, *Fractures and Fracture Networks* (Kluwer Academic Publishers, Dordrecht, 1999).
[2] Z. Neda, R. Florian, and Y. Brechet, Phys. Rev. E **59**, 3717 (1999).
[3] O. Huseby, J.-F. Thovert, and P. M. Adler, J. Phys. A **30**, 1415 (1997).
[4] V. V. Mourzenko, J.-F. Thovert, and P. M. Adler, Phys. Rev. E **72**, 036103 (2005).
[5] I. Balberg, C. H. Anderson, S. Alexander, and N. Wagner, Phys. Rev. B **30**, 3933 (1984).
[6] L. A. Santalo, *Integral Geometry and Geometric Probability* (Addison Wesley, Reading, MA, 1976).
[7] R. Schneider and W. Weil, *Integralgeometrie* (Teubner, Stuttgart, 1992).
[8] T. Kihara, Rev. Mod. Phys. **25**, 831 (1953).
[9] J. S. Ketchel and P. M. Larochelle, J. Mech. Des. **130**, 092305 (2008).
[10] D. Stauffer and A. Aharony, *Introduction to Percolation Theory* (Taylor and Francis, Bristol, PA, 1992).